Characterization of Nonlinear Ultrasonic Waves Behavior while Interacting with Poor Interlayer Bonds in Large-Scale Additive Manufactured Materials

Sina Zamen[a], Ehsan Dehghan-Niri[a,*], Helem Al-Beer[a], John Lindahl[b], and Ahmed Arabi Hassen[b]

[a]*Intelligent Structures and Nondestructive Evaluation (ISNDE) Laboratory, Civil Engineering Department, New Mexico StateUniversity, Las Cruces, NM, USA*

[b]*Materials Science and Technology Division (MSTD), Oak Ridge National Laboratory (ORNL), Oak Ridge, TN, USA*

Abstract

Over the past decades, researchers have developed several nonlinear ultrasonic techniques for quality control of materials commonly used in different applications. Owing to the superior sensitivity of nonlinear ultrasound waves to small defects such as micro-cracks, their applicability in different nondestructive testing (NDT) problems has been investigated in numerous studies. These studies utilize frequency domain analysis to detect the generation of higher harmonics because of the formation of defects in the inspected medium. Frequency domain analysis based on the Fourier transform is a significant approach used in linear systems; however, it may not perform adequately on nonlinear systems. Hence, studies on nonlinear dynamics and physics consider analyzing systems' behavior in the phase-space domain. In contrast to the frequency domain analysis, which can result in information loss, analysis in the phase-space domain retains all the information regarding a system's states. In this study, the nonlinearities induced by poor interlayer bonding in polymer-based additive manufactured parts in the phase-space domain are investigated. It is convenient to characterize the nonlinearity in the phase-space domain because it provides a geometrical representation of a system's states. Two types of low quality interlayer bond are considered. The first type is simulated artificially while the second type is manufactured by reducing the bond quality during the printing process. The analysis verified that the received ultrasonic signals exhibit classical nonlinear behavior in the phase-space domain while interacting with simulated poor interlayer bonds. In addition, the results showed that the behavior of ultrasonic waves is amplitude-dependent and evolves into models that have not been previously reported. Furthermore, Largest Lyapunov Exponent (LLE) is used to quantify the behavior of nonlinear ultrasonic waves while interacting with poor interlayer bonds. Using LLE, it was observed that the divergence rate of the phase-space trajectories depends on the amplitude of the excitation. This observation quantitatively proves that nonlinear behavior of ultrasound while interacting with poor interlayer bonds can be amplitude-dependent. The results of both simulated and inherent poor interlayer bond cases showed that LLE can be used as a reliable quantitative damage-sensitive feature to detect and potentially characterize weak bonds, which are difficult to detect using conventional approaches. In addition, the reported results in the phase-space domain provide a basis for proposing a new mathematical model for ultrasonic waves interacting with poor interlayer bonds.

Keywords:

Classic Nonlinearity, Contact Acoustic Nonlinearity, Interlayer Bonding, Additive Manufacturing, Phase-Space.

*Corresponding author:
Email address: niri@nmsu.edu (Ehsan Dehghan-Niri)

1. Introduction

Additive manufacturing (AM) is an emerging research topic in industry and academia owing to the advantages of rapid prototyping, flexibility in material properties, reduction in cost, an overall enhanced design, and manufacturing sector efficiency [1]. Polymer and metallic-based AM is used in several applications for building complex components in power, automotive, oil and gas, and aerospace industries [2]. Components that are manufactured using AM processes should be extensively examined to identify any existing defects that would render them non-functional. These defects include porosity, residual stresses, and poor interlayer adhesion. A significant demand exists in the field of quality control, particularly in nondestructive testing (NDT), to develop new techniques to overcome the limitations of conventional quality control, and characterize and detect defects in AM components.

The first type of defect is porosity, which is the presence of voids (microvoids and macrovoids) in polymer-based AM. Microvoids occur in a printed bead as a result of air trapped in the feedstock and during the mixing of polymer melt. Macrovoids are large diamond-shaped voids that occur between adjacent beads with a circular cross-section [2]. The AM components exhibit different properties in different directions owing to the anisotropic nature of the deposition process. Mechanical anisotropy is often observed within the boundaries of adjacent layers, creating regions with maximum residual stresses [3]. Another type of defect occurs because of the layered production of AM processes, where residual stresses tend to form around the boundaries of each layer (weak regions). Most AM processes produce the components in a heated chamber setup, which results in a high thermal gradient that adds to the residual stresses. Residual stresses lead to distortion, warpage, and microcracking [2]. Poor interlayer adhesion is a type of defect that occurs owing to improper bonding between layers in the AM. Appropriate bonding occurs by local re-melting of the solidified layers with the newly deposited layer. The deposition temperature and thermal properties of the feed stock material are the two major factors that control interlayer bonding. Layer time varies depending on the type of polymer used [4].

The interlayer bond weakness has undesirable limitations with respect to the practical implications of AM components [5]. An important challenge in the nondestructive evaluation of AM components is the ultrasonic assessment and characterization of weak interlayer bonding [6]. The residual stress in poor interlayer bonds poses an additional challenge to the detection process of weak interlayer bonds using ultrasonic testing [7]. Consequently, detecting and evaluating poor interlayer bonds using conventional linear ultrasonic approaches are difficult as the transmitted wave does not have sufficient energy to exhibit detectable changes in linear features such as amplitude owing to the change in stiffness. In contrast, a high-power ultrasonic approach can cause nonlinear behavior of ultrasonic waves when interacting with weak interlayer bonds.

Nonlinear ultrasonic testing has become popular in the field of NDT because it is more attuned to detecting small defects, such as microcracks, when compared with conventional ultrasound testing. Large wave amplitude and traveling long distances are two fundamental factors that can enhance nonlinearities in ultrasonic waves [8]. Two different classes of nonlinear models that are widely used to explain nonlinear ultrasound behavior are: 1. The classical nonlinear theory, which relies on the generation of higher harmonics, and 2. Non-classical nonlinear theories [8]. The classical nonlinear theory of elasticity considers Hooke's law with higher-order elastic terms [8]. Non-classical models are used owing to an assumption that the stiffness is asymmetric across the near-surface of a bond or crack interface [9]. Based on this assumption, contact acoustic nonlinearity (CAN) models have been proposed. Models based on bi-linear stiffness (stiffness asymmetry) are some of the most popular and simple nonlinear models [8, 9, 10]. A bi-linear nonlinear model has successfully used to represent breathing cracks given that the stiffness of the system changes with the position of the two faces of the crack. When the crack experiences tension, it opens, which results in global stiffness reduction; however, when it is under compressive loads, the crack closes, and the global stiffness of the system remains constant.

Most of the reported research in the nonlinear ultrasonic field relies on the generation of higher harmonics in the frequency domain [8, 11]. Analyzing ultrasonic waves in the frequency domain is a common approach and has been used in several studies to analyze different disbonds and imperfect interfaces successfully [7, 12, 13, 14, 15, 16, 17]. Furthermore, nonlinear ultrasound has also been used in defect evaluation of parts manufactured with AM processes. The feasibility of online ultrasound measurement using ultrasonic testing during the selective laser melting process has been demonstrated by Rieder et al. using time and frequency domain analysis of received ultrasound signals [18, 19]. Ultrasound testing has been used successfully for quality control of metal and plastic based additive manufactured parts [20, 21, 22, 23]. The ultrasonic tests have been successfully conducted on samples made from powdered-aluminum alloy, and AlSi10Mg samples manufactured by selective laser melting (SLM) with implanted defects [24, 25]. Also, immersion ultrasonic testing has been performed on 3D printed samples made from acrylonitrile butadiene styrene (ABS) by fused deposition modeling (FDM) [26]. While the frequency domain successfully used in several application using nonlinear ultrasound, analyzing a system response in the frequency domain using the Fourier transform has several shortcomings [27, 28]. The Fourier transform divides the signal into individual harmonic signals with different frequencies. Because the Fourier transform is a linear function, the Fourier transform of nonlinear systems changes a set of complex differential equations into integral equations in the frequency domain with convolutions among dependent variables [27]. Thus, studies are being conducted to enhance the frequency-based methods [29] or suggest new approaches to analyze a system response [27]. A well-known and effective method for analyzing system behavior is the phase-space analysis. The phase-space analysis provides a powerful domain for analyzing the complex nonlinear behavior of dynamic systems and physical phenomena [30].

By plotting systems' independent states with respect to each other, it is possible to construct and depict the systems' behavior in the phase-space domain with unique geometric features. In this domain, time is implicit. The phase-space domain enables visualization of the system behavior. Furthermore, because of the unique geometric representation of a dynamic system in this domain, different signal processing techniques and mathematical tools can be utilized to analyze a system's nonlinear response. Recurrence quantification analysis (RQA) can be used to demonstrate the determinism of a system behavior [30, 31, 32]. In other words, it is possible to determine if a system behavior is stochastic or deterministic. The instability of a system can be quantified by calculating the Lyapunov exponent. A fractal dimension analysis can be used to assign dimensions to a system behavior geometry. In addition, the phase-space domain analysis is a powerful method for determining chaotic motion and studying the system behavior transition to chaos [30, 31, 32].

Recently, studies in the ultrasonic field have utilized the phase-space domain to analyze signals and assess damages. Carrión et. al. [33] implemented RQA to assess the damage severity effect on system behavior in concrete materials. They concluded that by increasing the damage level and with higher frequency ultrasonic waves, the determinism of a system decreases significantly. This implies that the system behavior transforms from a deterministic behavior to stochastic behavior [33]. Dehghan-Niri and Al-Beer used the phase-space reconstruction to categorize the interaction of nonlinear ultrasonic waves with closed interfaces on high-strength aluminum material [34]. In the phase-space domain, Zamen and Dehghan-Niri applied different signal processing techniques to verify the chaotic motion of nonlinear ultrasonic waves while interacting with a closed interface crack due to residual stress in concrete materials [35]. Additionally, they used fractal dimension analysis to extract a quantitative damage-sensitive feature from nonlinear ultrasonic wave in the phase-space domain [36, 37].

The main contribution of this study is to propose a method to classify behavior of nonlinear ultrasonic waves imposed by the poor interlayer bond in AM components; the method should be convenient and reliable without relying on the frequency domain response. Because the phase-space approach considers all possible states of a system, it would result in superior accuracy when compared with the frequency domain-based approaches. In addition, the phase-space representation provides geometrical information that facilitates easy interpretation of complex data. Furthermore, to quantitatively identify ultrasonic waves behavior when interacting with poor interlayer bond, Largest Lyapunov Exponent (LLE) [38] is used. Lyapunov exponent measures the rate of divergence and convergence of system's trajectories in the phase-space domain, locally. Since for a dynamical system, there exists a spectrum of Lyapunov Exponents [31], maximum value is selected to represent the maximum amount of divergence or convergence in received ultrasound signals. The paper is further organized as follows: Section 2 presents a brief discussion on phase-space reconstruction of recorded data. In addition, the phase-space representation of well-known nonlinear models is presented. Section 3 presents the experimental setup of this study. The results and discussions are presented in Section 4, and the conclusions are presented in Section 5.

2. Methodology

2.1. Phase-Space Reconstruction of Nonlinear Ultrasonic Models

This section introduces the phase-space domain fundamentals, well-known ultrasonic models, and their corresponding behavior in the phase-space domain. To transform ultrasonic signals ($X(t)$) from the time domain to the phase-space domain, the delay method proposed by Packard et al. [30, 31, 32, 39] was used. The delay method is based on calculating the embedding dimension (E) and time lag (τ). $X(t)$, which represents the displacement or pressure fields of the ultrasonic waves, is one state of the system (S). Hence, $X(t)$ which is a discrete scalar value, can be obtained as $X(t) = S(x(t))$ where $x(t)$ is the input. Using the delay method, the phase-space representationof the ultrasonic signal can be defined as:

$$\boldsymbol{W} = (w_1, w_2, ..., w_E), \tag{1}$$

where $w_E(t) = X(t - (E - 1)\tau)$ [36]. To calculate the embedding dimension, the false nearest neighbors introduced by Kennel et. al. [40] was used. Additionally, to determine the time lag, the average mutual information introduced by Fraser and Swinney was used [41]. In this section, the time lag value (τ) and embedding dimension (E) for all models are considered as 0.25 T and 2, respectively. Before discussing the conventional nonlinear ultrasound models, a linear ultrasound waveform, its frequency domain, and phase-plane (2-dimensional phase- space) representations are illustrated in Fig. 1.

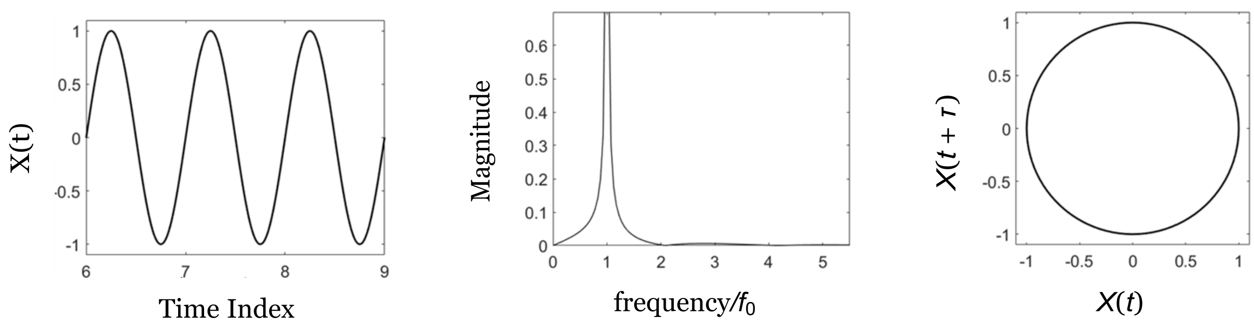

(a) Time domain (b) Frequency domain (c) Phase-plane

Fig. 1: Frequency domain and phase-plane evolution of linear wave form [34].

The recent research paradigm in the nonlinear ultrasound field divides acoustic nonlinearity as ‘classical nonlinear theory’ and ‘non-classical nonlinear theory’. The classical nonlinear theory is based on Hooke’s law and accounts for higher-order elastic terms [8]. The quadratic (Fig. 2) and cubic (Fig. 3) nonlinear models are the most commonly used models in classical acoustic nonlinearity research [34].

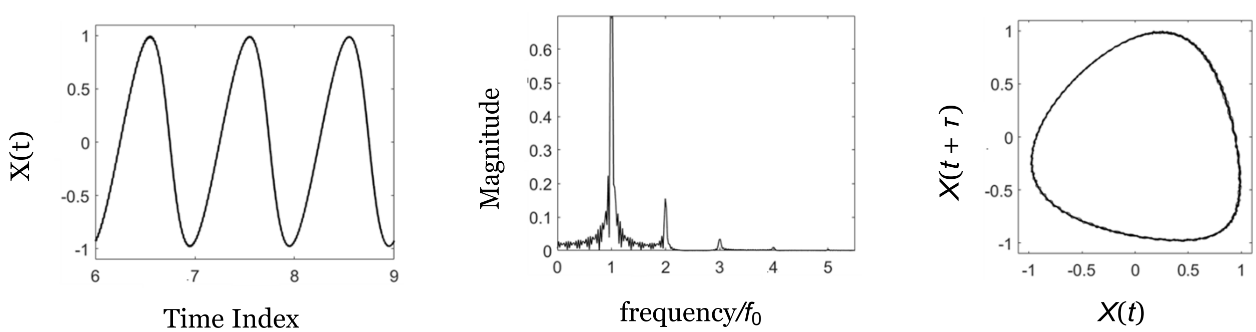

(a) Time domain (b) Frequency domain (c) Phase-plane

Fig. 2: Frequency domain and phase-plane evolution of wave form with quadratic nonlinearity term [34].

While classical nonlinear theory can be successfully applied for approximately homogeneously distributed damage it has limitations to be used for localized defects. CAN model, however, is caused by the contrasting behavior of the tension and compression portions of ultrasound waveforms in the region of localized defects within interfaces that

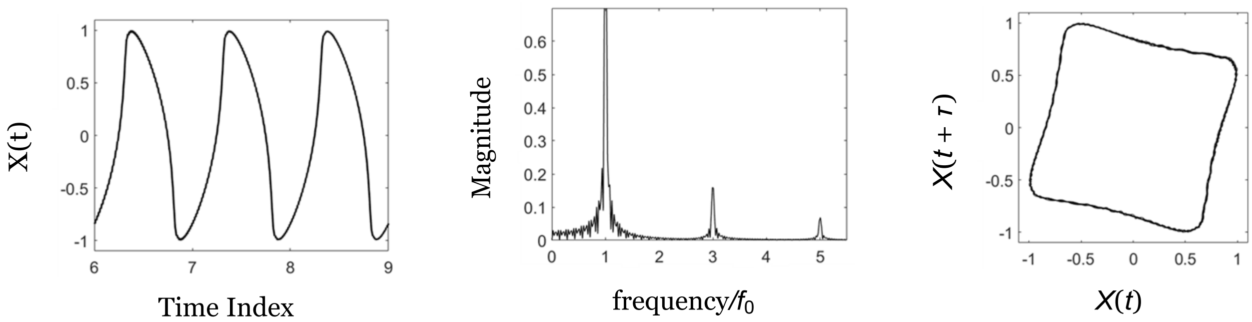

(a) Time domain (b) Frequency domain (c) Phase-plane

Fig. 3: Frequency domain and phase-plane evolution of wave form with cubic nonlinearity term [34].

are in contact. The compression component part of the wave can penetrate through the defect region, whereas the tensile portion cannot effectively penetrate through it. Since this phenomenon was first observed in 1978 [42], there have been numerous investigations on its application in the detection and characterization of imperfect interfaces and cracks [43, 44, 45, 46]. A popular nonlinear model for non-bonded contact interfaces that can address CAN is a simple bi-linear stiffness model [47], also known as stiffness asymmetry [9], which is shown in Fig. 4. This model has been used to address the clapping mechanism observed during wave interaction with cracks [48, 49]. The CAN has been used to evaluate kissing bonds in adhesive joints [7].

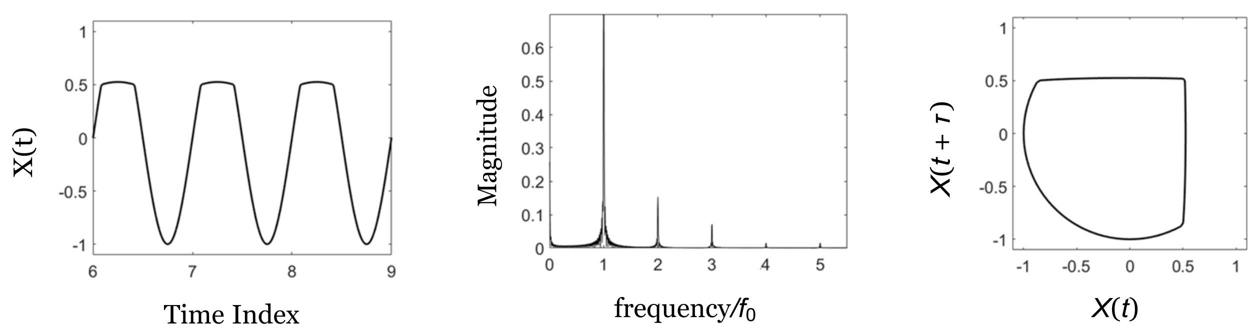

(a) Time domain (b) Frequency domain (c) Phase-plane

Fig. 4: Frequency domain and phase-plane evolution of bi-linear wave form [34].

Another nonlinear acoustic model observed is hysteresis. The hysteresis depends on the condition of the material and its loading history [8]. However, hysteresis behavior of acoustic nonlinearity lacks a theoretical foundation regarding its origin. Following a different path and returning to the origin (end-point memory) in the stress–strain domain could be an indicator of hysteresis behavior in a material [8, 34]. This behavior is shown in Fig. 5.

Other mathematical models for nonlinear acoustic phenomena induced in solids exist in the literature. Most of the models rely on the frequency domain. As previously indicated, the frequency domain can be a valuable tool for analyzing linear systems with the advantage of switching back to the time domain from the frequency domain using its inverse feature. Nevertheless, the existing literature confirms that the frequency analysis is not always suitable for nonlinear system analysis and in some cases cannot be successfully used [27]. The phase-space domain

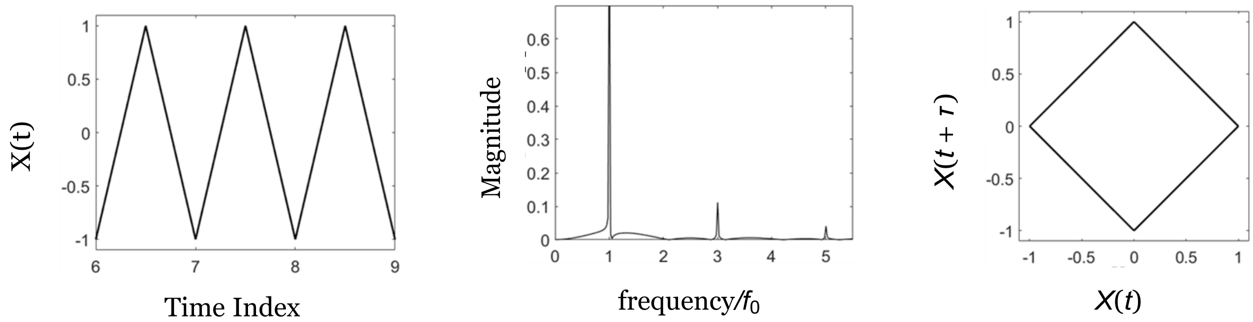

(a) Time domain　　Frequency domain　　(b) Phase-plane

Fig. 5: Frequency domain and phase-plane evolution of hysteresis wave form [34].

preserves all the states of a system and enables the analysis of the system behavior using different signal processing techniques.

2.2. Largest Lyapunov Exponent

After constructing the phase-space representation of ultrasonic signals, a quantitative feature that can measure the exponential divergence of initially close state-space trajectories can be extracted. LLE calculates the largest divergence of trajectories in the phase-space domain. Let $s(t_1)$ and $s(t_2)$ be two point in state space with distance $|s(t_1) - s(t_2)| = \delta_0 << 1$. To calculate the distance between the two trajectories ($\delta_{\Delta t}$) passing through these points at Δt time steps ahead, the following equation can be used:

$$\delta_{\Delta t} \simeq \delta_0 e^{\lambda \Delta t}, \qquad \delta_{\Delta t} \ll 1, \qquad \Delta t \gg 1. \tag{2}$$

where λ is the Lyapunov exponent. Positive values of λ denote the divergence of the trajectories in the phase-space domain while negative values of λ verify their convergence. λ equal to zero shows that trajectories are evolving in the phase-space domain without changing their distance with respect to each other. For calculating LLE, an algorithm proposed by Rosenstein et al. [38] and Kantz [50] was used. This algorithm measures the average separation of neighbors without normalizing them. Finally, the algorithm fits a line to the data using the least-squares method. First, the algorithm calculates the following values:

$$S(\Delta t) = \frac{1}{N} \sum_{t_0=1}^{N} ln(\frac{1}{|U(s_{t_0})|} \sum_{s_t \in U(s_{t_0})} |s_{t_0+\Delta t} - s_{t+\Delta t}|) \tag{3}$$

where s_{t_0} is a data point of the the times series in the phase-space domain. $U(s_{t_0})$ is the neighborhood of s_{t_0} with diameter E. The size of the neighbourhood should be as small as possible but also large enough so each point has a couple of neighbours [50]. Since the optimal value of sigma is unknown, $S(\Delta t)$ should be computed for a variety of E values. The slope of the part of the function $S(\Delta t)$ where it is linearly increasing is the LLE value.

In the next section, the experimental setup used in this research is described.

3. Experimental Setup

A big area additive manufacturing (BAAM) system at the U.S. Oak Ridge National Laboratory was used in this work. The BAAM system deposition head is shown in Fig. 6. It is a four-heating zone single-screw polymer extruder mounted on a large gantry system with a build volume of 6 m in length, 2.5 m in width, and 1.8 m in height. In the extrusion deposition process used in BAAM, a semi-molten polymer is extruded through a nozzle mounted at the end of the extruder and deposited layer-by-layer. The material used to fabricate the samples was acrylonitrile butadiene styrene (ABS) reinforced with 20 wt% carbon fibers supplied by Techmer ES. The printing parameters and extruder temperatures are listed in Table 1. The bed temperature was maintained at 110 °C to assist with initial layer adhesion. A hollow hexagon with a side length of 457.2 mm, wall thickness of 140 mm, and height of 114.5 mm was printed. Then, several 101.6 mm cubic samples were extracted from the hexagon through a milling process.

To perform the ultrasound test, two types of low quality interlayer bond were considered. The first type was simulated artificially while the second type was manufactured by reducing the bond quality during the printing process. In the simulated defect case, the samples were placed in a compression tool, as shown in Fig. 7. This tool was fabricated to produce loaded contacting interfaces, while accessing both sides of the samples to excite and receive the ultrasound. The load on the samples can be controlled and applied by tightening the nuts at the ends of the two threaded high-strength steel rods that connect the two solid caps using a torque wrench. A data acquisition board with a Labview program was used to measure the applied compressive load from the two precise load cells (FUTEK LTH400) at the other ends of the rods. To mimic a poor interlayer bond, two cube samples were placed in the compression tool and loaded with a pressure of 15 kPa. A liquid polymer (C_nH_{2n+2}) with 0.1 mm thickness was placed between the samples to better simulate the defect [7].The second type of defect was introduced in the BAAM using a different speed and the same printing parameters and extruder temperatures mentioned in Table 1. The layer time was increased to 196 seconds to allow layers to get cold before the deposition of a new layer. The layer time refers to the time interval of one complete layer extrusion deposition. Hence, the bond quality between layers was reduced. Three cases were considered: 1. A sample with perfect interlayer adhesion, 2. A sample with a simulated poor interlayer bond and 3. A sample with inherent poor interlayer bond.

An arbitrary wave generator was used to generate a sinusoidal signal. To acquire the desired high voltage excitation, the initial signal was amplified by 26 dB (e.g. increasing amplitude by 20 times) using a high-power amplifier (excitations with peak-to-peak amplitudes of 90-170 V with 10 V increments are used). A 21-cycle sinusoidal signal (Fig. 9) with a center frequency of 500 KHz is excited using a resonance 25.4 mm (1 inch) diameter piezoelectric contact transducer (Panametrics) to provide a sufficiently long steady signal. Another reason for selecting the number of cycles equal to 21 was to avoid tail effect which can cause the generation of subharmonics [51]. The smallest cubic sample dimension in this experiment was 0.1016 m. Since the ultrasonic waves speed in polymer material is around 2000 m/sec, the travel time of the excited wave from one side of the sample to the other side is equal to 50.8 μs. Hence a relatively small excitation time was selected by limiting the number of cycles to avoid the tail effect. On the other side of the samples, a broad- band 25.4 mm (1 inch) diameter piezoelectric contact transducer (Panametrics) with an effective frequency of 500 KHz is used as a receiver to record the received waveform. The frequency bandwidth of the receiver transducer is not wide enough to cover the fifth harmonic. For capturing signals, a LeCroy WAVERunner 6050A oscilloscope with a sampling frequency of 50 MHz and variable sensitivity of $2mV - 10V/div$ were used. The large-diameter transmitter is used for two reasons: 1. to input higher ultrasound energy and enhance the signal-to-noise ratio (SNR), and 2. for a smaller beam spread angle to avoid

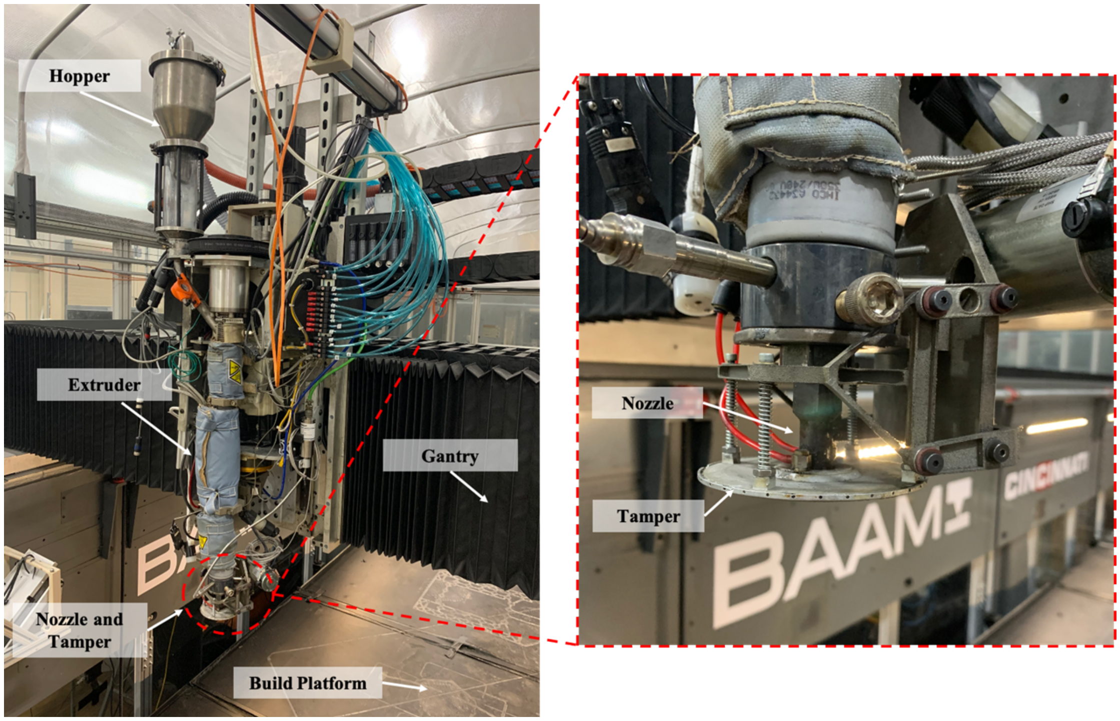

Fig. 6: The BAAM system deposition head.

side interference at the receiver point. The sample width is sufficiently large to avoid any side interference. Because the SNR is enhanced, amplifying the received waveform is not required, which can reduce the nonlinearity due to electronics. The experimental setup is shown in Fig. 7 and a schematic representation of it is displayed at Fig. 8.

The next section presents the behavior of ultrasonic waves while interacting with poor interlayer bonds in the time, frequency and phase-space domains.

4. Results

4.1. Sample with simulated poor interlayer bond

Here, the time and frequency domain analysis as well as phase-space representation of the received ultrasound signals of the intact sample and the sample with the simulated defect are presented. Fig. 10 presents the windowed time domain response and frequency responses of the received ultrasonic signal with excitation amplitude of 170 V for the intact sample. From the time domain response of the intact sample, a simple harmonic response is observed. Additionally, according to the frequency domain analysis, no higher harmonics are detected. This can imply the linear behavior of ultrasonic waves in the intact sample. Furthermore, it highlights the fact that the testing setup does not have an inherent source of nonlinearity.

Fig. 11 shows the time domain responses of the received ultrasonic waves of the defected sample with different excitation amplitudes. A small window (20 μs) of received ultrasonic waves is used to better illustrate the nonlinear behavior of these waves in the time domain. For the data analysis, however, the full length of the signals was used. Observed asymmetric response specially for larger voltage implies a different displacement field for tension and compression. This observation is similar to bi-linear nonlinear model shown in Fig. 4. However, there is a

Table 1: Printing parameters and extruder temperatures

Printing parameters	
Layer Height (mm)	3.8
Bead Width (mm)	8.5
Nozzle Diameter (mm)	7.6
Gantry Speed (mm/sec)	276.4
Number of Layers	30
Screw Speed (RPM)	300
Layer Time (Sec)	98
Total Print Time (Min)	50
Zone 1 Temperature (°C)	177
Zone 2 Temperature (°C)	177
Zone 3 Temperature (°C)	205
Zone 4 Temperature (°C)	232
Zone (Tip) Temperature (°C)	250

noticeable difference in the observed and bi-linear responses in the time domain. Although, the distortion of signals potentially caused by nonlinear behavior is observed from Fig. 11, it is not possible to classify the cause of these distortions. As mentioned earlier, the time domain response is not a reliable source for model classification as well as defect characterization.

Fig. 12 demonstrates the frequency analysis of the received ultrasonic wave of the defected sample excited with 90 V amplitude. In Fig. 12, no higher harmonics are observed. Fig. 13 presents the frequency domain analysis of the received ultrasonic waves in the defected sample excited with amplitudes of 100-140 V. The initiation of the third-harmonic generation is observed in classical nonlinearity models, bi-linear models, and hysteresis models. However, the third-harmonic generation in the aforementioned models is accompanied by the generation of other harmonics. In contrast, in Fig. 13, the first and third harmonics are the only observed higher harmonics. Furthermore, this result cannot be explained using bi-linear model because in this model the generation of the second harmonic prior to the generation of the third harmonic was expected. Furthermore, in the bi-linear model the second harmonic had a larger amplitude when compared with the third harmonic. However, in Fig. 13, the generation of the second harmonic is not observed.

The generation of higher harmonics in the frequency domain is expected with an increase in the amplitude of ultrasonic waves. In Fig. 14, as the amplitude of excitation increases, the fourth and second harmonics are observed in the frequency domain. The aforementioned harmonics (or generation of the first four harmonics) with the observed relative amplitudes have not been explained previously using any of the mathematical nonlinear models. As mentioned earlier, the frequency domain is unreliable because by transferring nonlinear data to the frequency domain, important information about the states of a nonlinear system may be lost. Consequently, the behavior of ultrasonic waves—while interacting with a poor interlayer bond—in the phase-space domain is investigated. Before

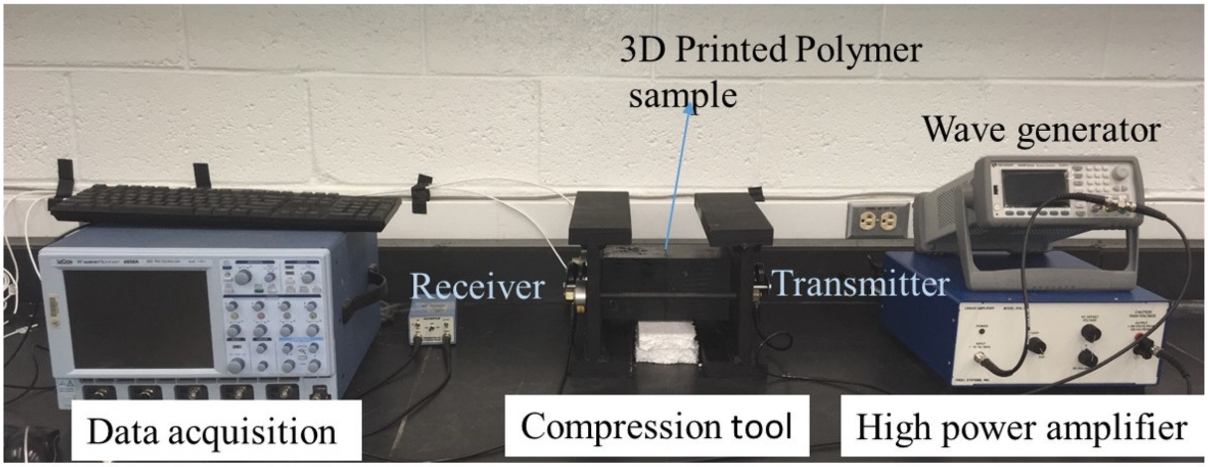

Fig. 7: Experimental setup showing the compression tool and ultrasound testing system.

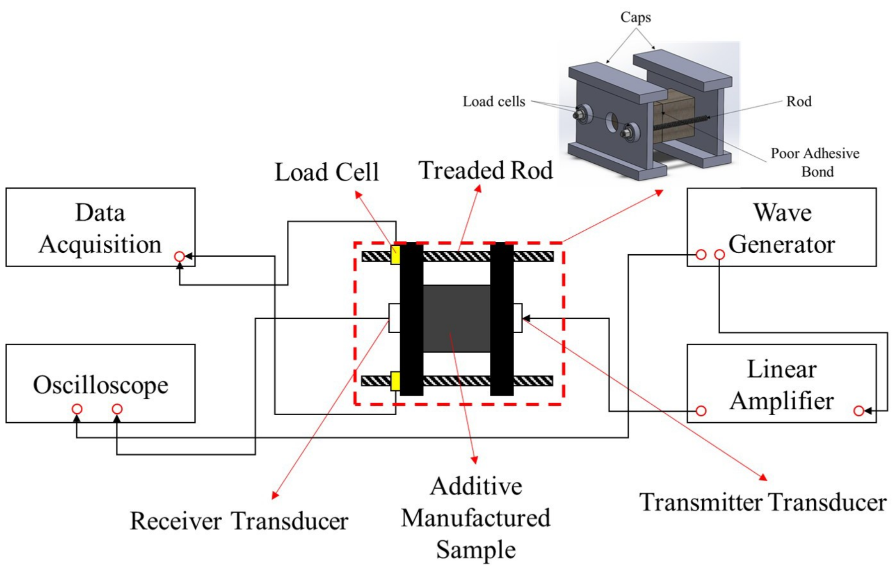

Fig. 8: Schematic representation of experimental setup showing the compression tool and ultrasound testing system.

constructing the phase-space domain, two important variables should be determined: embedding dimension and time lag. Using the methods mentioned in Section 2, embedding dimension for all received signals calculated to be 2. Further, using the average mutual information theory, the time lag ratio for each signal was calculated. The minimum value of each curve in Fig. 15 is considered as the time lag ratio, which is required for generating phase-space representation.

As the phase-space analysis transfers data to a new domain without potentially losing information [27, 50], the results based on the phase-space analysis can be used to complement the time domain and frequency domain analyses for more accurate and reliable damage detection or behavior characterization. The phase-space domain better retains and illustrates all possible states of the system. The phase-plane representation of the ultrasonic wave for intact sample is shown in Fig. 16. The circular trajectory of system's behavior in this domain is observed which verifies the linear behavior of ultrasonic wave. Also, the linear behavior of received ultrasonic signal can verify that

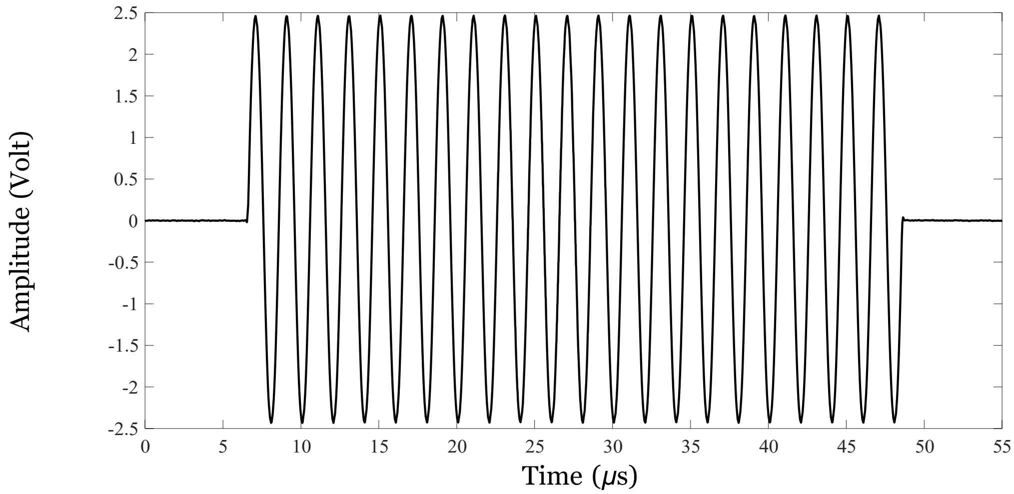

Fig. 9: Excited wave sample before amplification (21 cycles at the center frequency of 500 KHz).

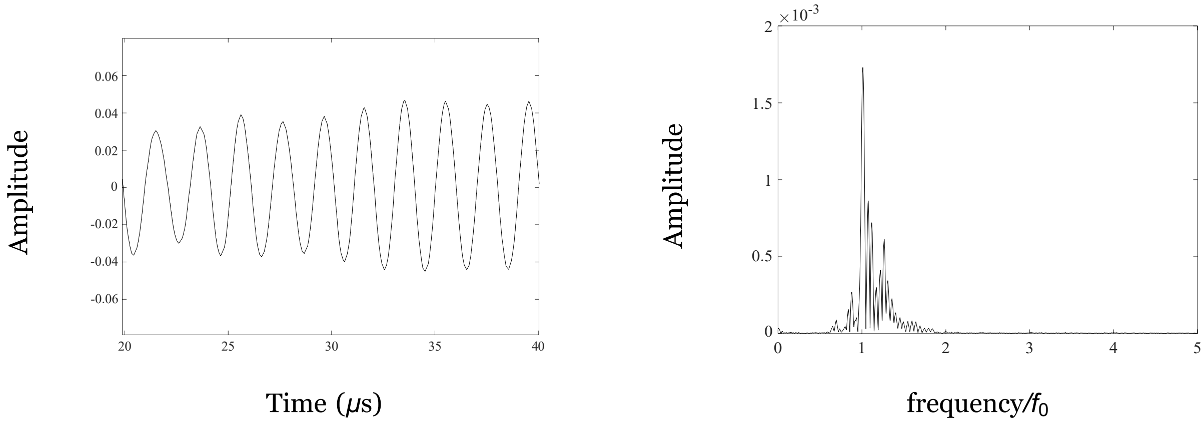

(a) Time domain

(b) Frequency domain

Fig. 10: Time and frequency domain of received ultrasonic signal for the intact sample.

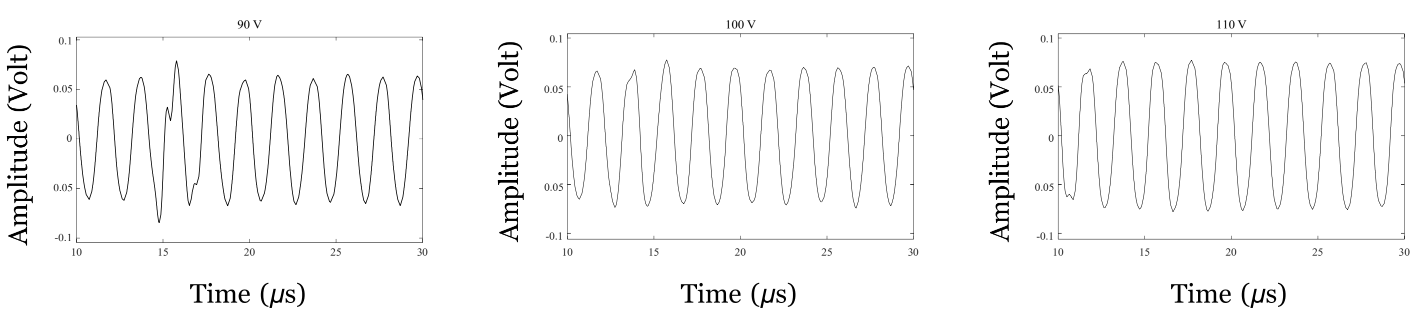

testing setup does not have unfavorble nonlinearity source to alter the result. The phase-plane representation of the ultrasonic waves of defected sample is shown in Fig. 17. Fig. 17 shows that the ultrasonic waves start their nonlinear behavior when excited with amplitudes of 90 V or more, as the phase-space representation of the waves are not circular any more for the defect sample. The nonlinear behavior of the ultrasound wave could not be verified for 90 V excitation in the frequency domain showing that the phase-space domain is more effective than frequency

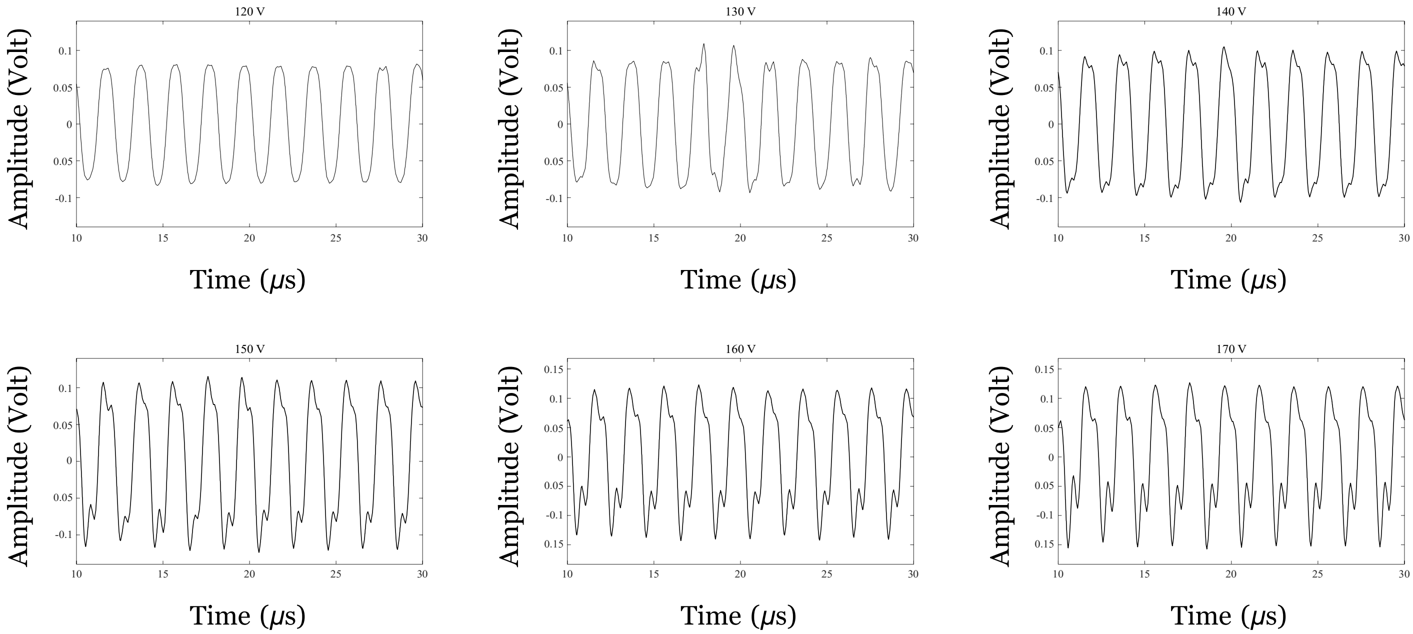

Fig. 11: Evolution of ultrasonic waves in the time domain.

domain in revealing this type of behavior. By increasing the amplitude of excitation, the behavior of the waves shifts to a classical nonlinear model with a cubic term. This behavior is discernible for ultrasonic waves with an amplitude up to 130 V. the classical nonlinear behavior transforms to a model with curved sides, which has not been reported previously. A classical nonlinear model with a cubic term has the first, third, and fifth harmonics.

Another advantage of the phase-space analysis is its sensitivity to the amplitude of excitation. Fig. 17, shows that a slight change in the excitation amplitude results in a noticeable change in the ultrasound wave behavior in the phase-space domain. This advantage can prove the phase-space analysis to be a suitable approach for monitoring weak adhesive bonds that are difficult to detect using the frequency domain analysis. While interpreting data in the frequency domain can be challenging, the phase-space representation of ultrasonic waves provides a geometric representation of their behavior. The linear and nonlinear behavior of these waves is easily discernible by the observer because the linear behavior forms a circle in the phase-space domain. The phase-space domain provides an easy and reliable classification tool distinguish nonlinear behaviors when compared with the frequency domain analysis. This accurate system behavior classification ability can enhance the mathematical modeling of the nonlinear behaviors.

Finally, for quantifying the behavior of nonlinear ultrasound waves while interacting with poor interlayer bond, LLE values with respect to amplitude of excitation for intact sample as well as defected sample are displayed in Fig. 18. Increasing trend of LLE values when excitation amplitude increases can be observed from Fig. 18 for defected sample. The larger value of LLE asserts that phase-space trajectories are diverging from each other with higher rate. On the other hand, for intact sample, the LLE values are significantly smaller than the LLE values obtained from the sample with poor interlayer bond. The LLE remains constant with increasing the amplitude of excitation. This result shows that LLE can be used as a reliable quantitative damage-sensitive feature to detect and potentially characterize weak bonds, which are difficult to detect using conventional approaches. Additionally, this observation quantitatively proves that nonlinear behavior of ultrasound while interacting with poor interlayer

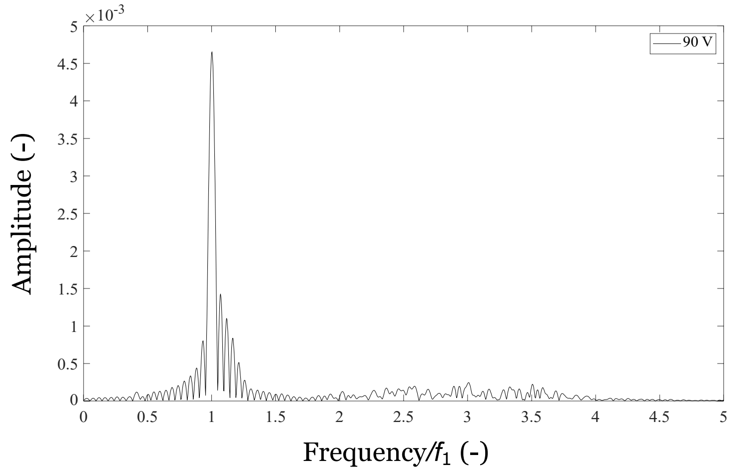

Fig. 12: Frequency response of received ultrasonic waves with amplitude of 90 V for defect sample.

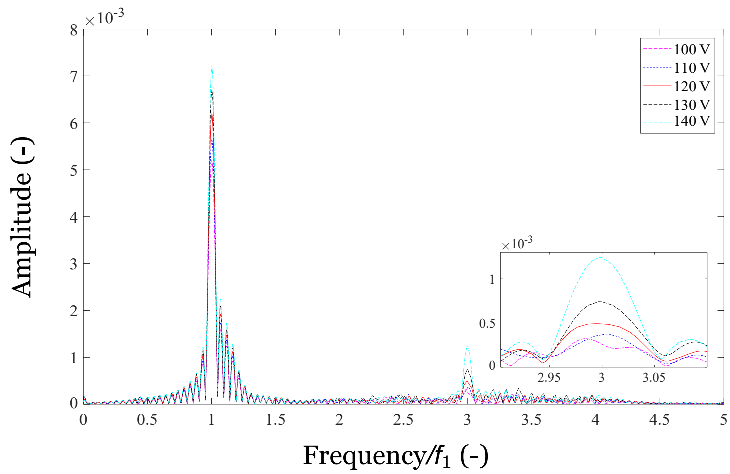

Fig. 13: Frequency response of received ultrasonic waves with amplitude of 100-140 V for defect sample.

bonds is amplitude-dependent.

4.2. Sample with inherent poor interlayer bond

In the inherent defect case, the results of ultrasonic testing with 170 V amplitude are shown in Fig. 19. In the same way as the intact sample, the results did not show dependency on amplitude. Hence, only the results of ultrasonic testing with 170 V amplitude were reported in Fig. 19. In Fig. 19 (b), frequency analysis of the received wave is displayed. Interestingly, the subharmonics can be seen in frequency domain response. According to [51], large-amplitude ultrasonic excitation can cause a nonlinear effect in the presence of closed cracks that can generate subharmonics in frequency domain response. The observation of subharmonics, in this case, can be used as a sensitive feature for quality control of the 3D printed materials. Also, as it is shown in Fig. 19, the phase-space trajectories for ultrasonic signals are completely different compared to the intact sample's trajectories. In contrast to the simulated case, the phase-space domain is not as useful as it was in the simulated case for model identification. It can, however, be used to quantitatively reveal inherent dynamic behavior of the system that cannot be readily determined in both time and frequency domains.

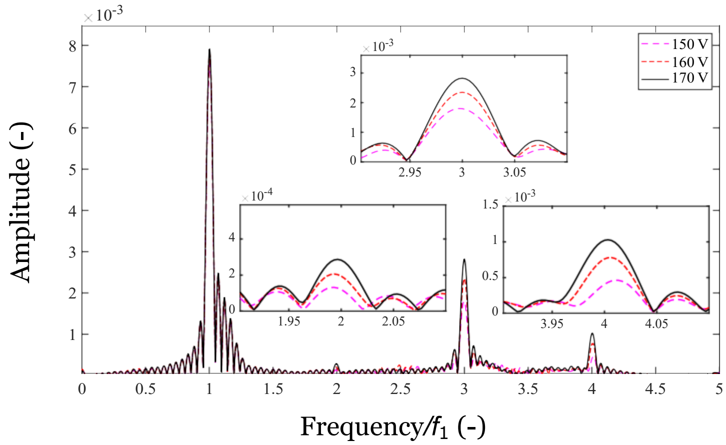

Fig. 14: Frequency response of received ultrasonic waves with amplitude of 150-170 V for defect sample.

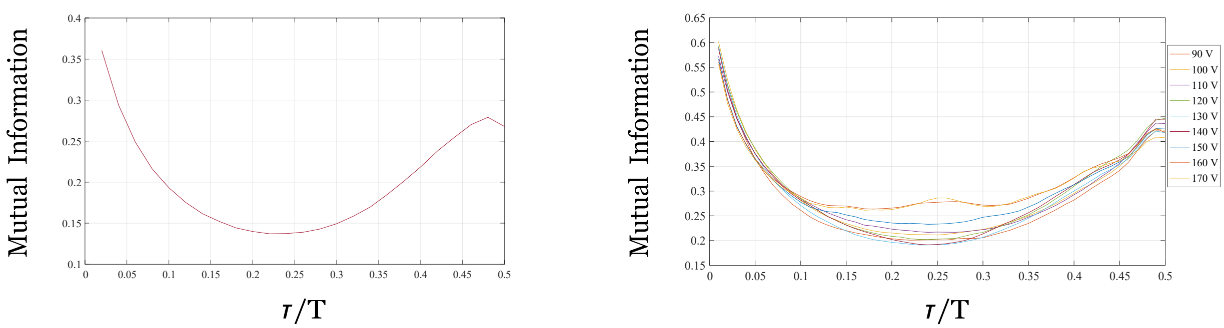

(a) Intact Sample (170 V)

(b) Defected Sample

Fig. 15: Time lag to excitation period ratio calculated by average mutual information for the received ultrasonic signals.

Additionally, LLE values were calculated for different amplitudes, and results are displayed in Fig. 20. sample with inherent poor interlayer bonds yields larger LLE values compared to the intact sample. This highlights the sensitivity of the phase-space domain to the sample's condition. The LLE value extracted from the phase-space domain is a reliable feature to characterize nonlinear ultrasonic waves behavior in additive manufactured parts with poor interlayers bonds. Comparing Fig. 18 and Fig. 20, one can observe that the increasing trend of LLE with respect to excitation amplitude is less pronounced in the sample with inherent poor interlayer bonds. This might be due to the fact that the simulated defect bond is much weaker compared to the sample with inherent poor interlayer bonds. It should be noted that in general for nondestructive testing applications, damage sensitive features that are less sensitive to the excitation amplitude are more reliable in detecting and evaluating defects.

5. Conclusion

This study considers the resulting nonlinear behavior in the phase-space domain of ultrasonic waves while interacting with poor interlayer bonds. Two different samples with poor interlayer bonds were considered. In the first case, two 3D-printed polymer cubic samples with a liquid polymer between them were used to simulate a poor interlayer bond. Then, the samples were placed inside a compressive tool that applies compressive force on both

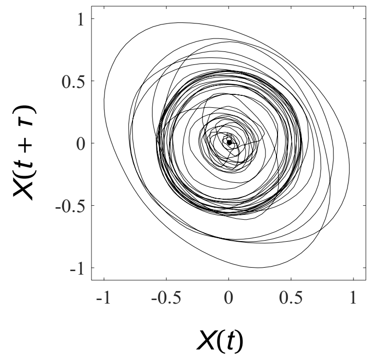

Fig. 16: Trajectories of ultrasonic wave in the phase-space domain for Intact sample (170 V).

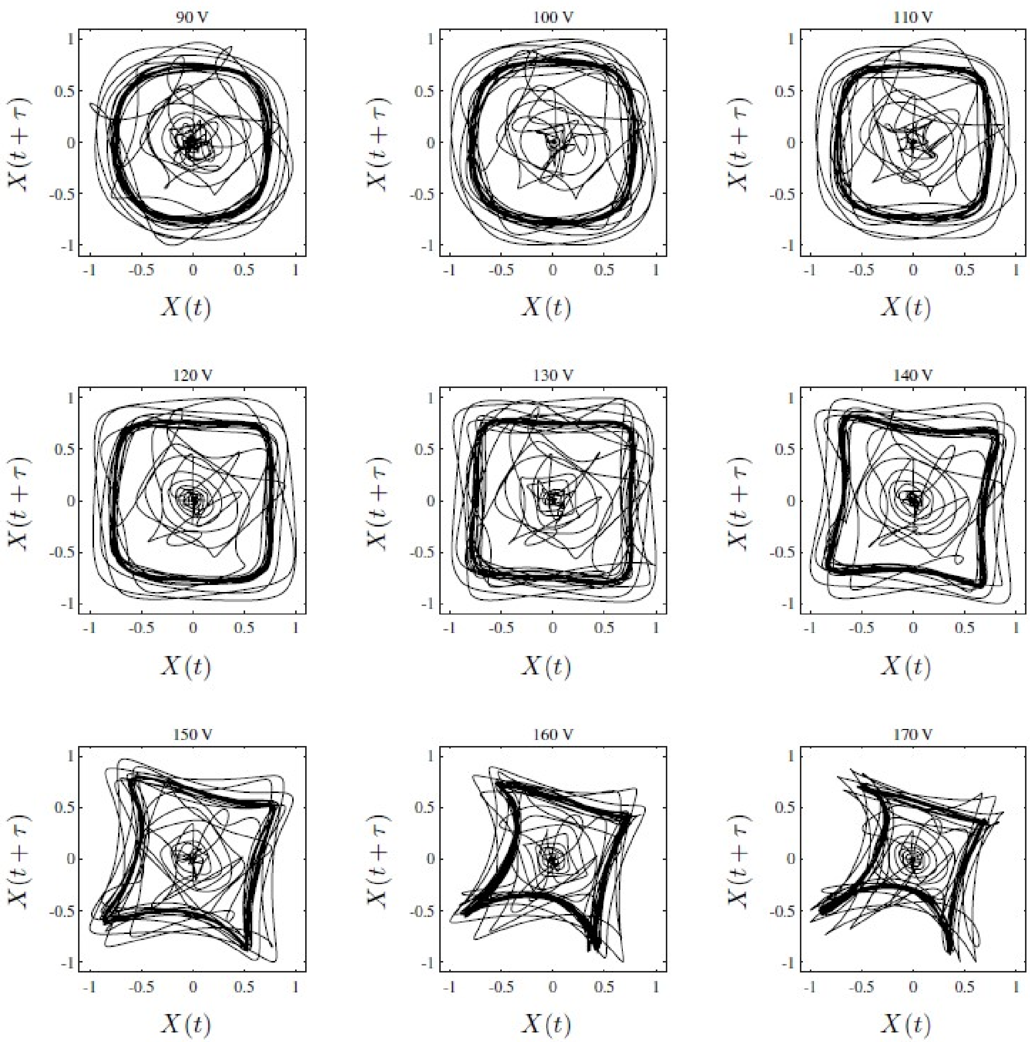

Fig. 17: Nonlinear Evolution of ultrasonic waves in the phase-space domain.

sides of the sample. Simultaneously, ultrasonic testing with different amplitudes was performed. For the second sample, the speed of printing process was intentionally decreased to create real poor interlayer bonds.

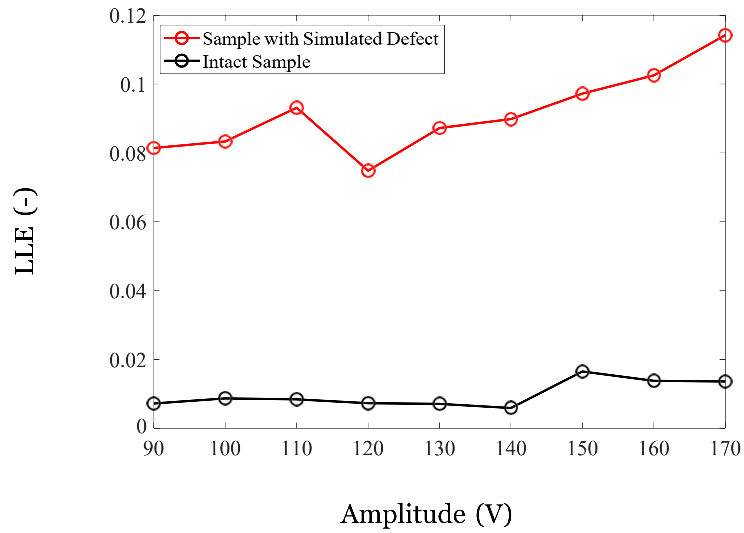

Fig. 18: Comparison of LLE values of the intact and defected samples.

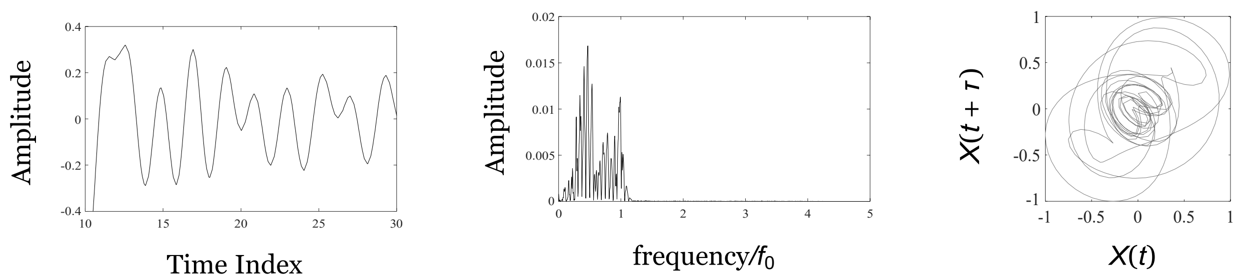

(a) Time domain (b) Frequency domain (c) Phase-plane

Fig. 19: Time domain, frequency domain and phase-plane evolution of ultrasonic wave form with 170 V amplitude for sample withweak interlayer bonds.

Contrary to the conventional approach of using ultrasonic waves in the frequency domain to study the ultrasonic wave behavior, the phase-space reconstruction of the received ultrasound signals was considered. The frequency domain analysis of the nonlinear systems in the first case was confirmed to be less sensitive method to study the behavior of the dynamical system, whereas the phase-space domain analysis of nonlinear dynamical systems can retain information regarding all possible states of the system.

The advantages of using the phase-space domain analysis of the received ultrasound waves were as follows. First, the phase-space domain analysis provided a geometrical representation of the system behavior. This helps in easily identifying subtle changes in the system behavior. Hence, the classification of a system's behavior and identifying abnormal behavior is straightforward. The frequency domain analysis relies on the generation of higher harmonics to identify or classify the behavior of a nonlinear system. Observation of higher harmanics can be significantly hampered for signals with low SNR. Second, the reported results for lower amplitude of excitation verify that the behavior of simulated poor interlayer bonds can be classified as a classical acoustic nonlinear model with a cubic nonlinearity term. This is important because it can be a strong foundation for generating mathematical models for

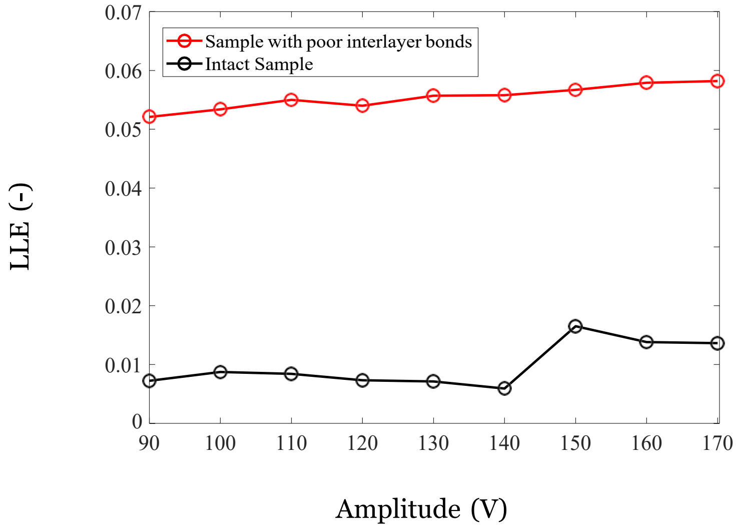

Fig. 20: Comparison of LLE values of the intact sample and sample with poor interlayer bonds.

this type of defects (e.g. poor interlayer bond). In addition, for larger excitation amplitude, the results show that the behavior of ultrasonic waves is amplitude dependent and evolves into models that have not been previously reported. Further, the ultrasonic waves trajectories rate of divergence in the phase-space domain calculated using LLE. The increasing trend of LLE values when increasing the excitation amplitude verifies that nonlinear ultrasound waves tend to diverge with higher rates while interacting with poor interlayer bonds at large excitation amplitude. Furthermore, this observation is another proof showing that nonlinear behavior of ultrasound while interacting with poor interlayer bonds is amplitude dependent. Additionally, the viability of the LLE as a damage-sensitive feature for the detection of poor interlayer bonds in polymer-based additive manufactured parts was shown.

In conclusion, although the frequency domain analysis is an important tool that provides insight into a system's initial behavior, it is important to analyze the system behavior in a powerful domain that considers all possible states of a nonlinear system. Utilizing mathematical tools such as recurrence analysis and Lyapunov exponent in the phase-space may provide more reliable and accurate tools for detection and evaluation of poor interlayer bonds in AM components.

Declaration of Conflicting Interests

The author(s) declared no potential conflicts of interest with respect to the research, authorship, and/or publication of this article.

Acknowledgments

We gratefully acknowledge the funding support from Department of Energy/National Nuclear Security Agency (Grant DE-NA0003987). Research was also sponsored in part by the U.S. Department of Energy, Office of Energy Efficiency and Renewable

Energy, Advance Manufacturing Office, under contract DE-AC05-00OR22725 with UT-Battelle, LLC. Large scale AM machine used in this research was sponsored by Cincinnati Inc., OH, USA. Feedstock materials used in this work were provided by Techmer PM., TN, USA.

References

[1] J. R. C. Dizon, A. H. Espera, Q. Chen, R. C. Advincula, Mechanical characterization of 3d-printed polymers, Additive Manufacturing 20 (2018) 44 – 67. doi:10.1016/j.addma.2017.12.002.

[2] A. A. Hassen, M. M. Kirka, Additive manufacturing: The rise of a technology and the need for quality control and inspection techniques, Materials Evaluation 76 (4) (2018) 438–453.

[3] S. C. Ligon, R. Liska, J. Stampfl, M. Gurr, R. Mülhaupt, Polymers for 3d printing and customized additive manufacturing, Chemical Reviews 117 (15) (2017) 10212–10290. doi:10.1021/acs.chemrev.7b00074.

[4] V. Kishore, C. Ajinjeru, A. Nycz, B. Post, J. Lindahl, V. Kunc, C. Duty, Infrared preheating to improve interlayer strength of big area additive manufacturing (baam) components, Additive Manufacturing 14 (2017) 7 – 12. doi:https://doi.org/10.1016/j.addma.2016.11.008.

[5] J. Allum, A. Moetazedian, A. Gleadall, V. V. Silberschmidt, Interlayer bonding has bulk-material strength in extrusion additive manufacturing: New understanding of anisotropy, Additive Manufacturing 34 (2020) 101297. doi:https://doi.org/10.1016/j.addma.2020.101297.

[6] P. B. Nagy, Ultrasonic classification of imperfect interfaces, Journal of Nondestructive Evaluation 11 (1992) 127–139. doi:10.1007/BF00566404.

[7] D. Yan, B. W. Drinkwater, S. A. Neild, Measurement of the ultrasonic nonlinearity of kissing bonds in adhesive joints, NDT & E International 42 (5) (2009) 459 – 466. doi:10.1016/j.ndteint.2009.02.002.

[8] D. Broda, W. Staszewski, A. Martowicz, T. Uhl, V. Silberschmidt, Modelling of nonlinear crack–wave interactions for damage detection based on ultrasound—a review, Journal of Sound and Vibration 333 (4) (2014) 1097 – 1118. doi:10.1016/j.jsv.2013.09.033.

[9] I. Solodov, N. Krohn, G. Busse, Can: an example of nonclassical acoustic nonlinearity in solids, Ultrasonics 40 (1) (2002) 621 – 625. doi:10.1016/S0041-624X(02)00186-5.

[10] K. Worden, Nonlinearity in structural dynamics: detection, identification and modelling, CRC Press, 2019.

[11] M. Deng, Modal analysis of second-harmonic generation of generalized lamb waves in layered planar structures, NDT & E International 38 (2) (2005) 85–95. doi:https://doi.org/10.1016/j.ndteint.2004.05.005.

[12] C. Brotherhood, B. Drinkwater, S. Dixon, The detectability of kissing bonds in adhesive joints using ultrasonic techniques, Ultrasonics 41 (7) (2003) 521 – 529. doi:10.1016/S0041-624X(03)00156-2.

[13] M. Rothenfusser, M. Mayr, J. Baumann, Acoustic nonlinearities in adhesive joints, Ultrasonics 38 (1) (2000) 322 – 326. doi:10.1016/S0041-624X(99)00083-9.

[14] D. Barnard, G. Dace, D. Rehbein, O. Buck, Acoustic harmonic generation at diffusion bonds, Journal of nondestructive evaluation 16 (2) (1997) 77–89. doi:10.1007/BF02683880.

[15] J. Alston, A. Croxford, J. Potter, P. Blanloeuil, Nonlinear non-collinear ultrasonic detection and characterisation of kissing bonds, NDT & E International 99 (2018) 105–116. doi:https://doi.org/10.1016/j.ndteint.2018.07.003.

[16] B. Yılmaz, E. Jasiūnienė, Advanced ultrasonic ndt for weak bond detection in composite-adhesive bonded structures, Int. J. Adhes. Adhes. 102 (2020) 102675. doi:https://doi.org/10.1016/j.ijadhadh.2020.102675. URL http://www.sciencedirect.com/science/article/pii/S014374962030138X

[17] B.-Y. Chen, S.-K. Soh, H.-P. Lee, T.-E. Tay, V. B. Tan, A vibro-acoustic modulation method for the detection of delamination and kissing bond in composites, J. Compos. Mater 50 (22) (2016) 3089–3104. doi:10.1177/0021998315615652.

[18] Q. Y. Lu, C. H. Wong, Applications of non-destructive testing techniques for post-process control of additively manufactured parts, Virtual and Physical Prototyping 12 (4) (2017) 301–321. doi:10.1080/17452759.2017.1357319.

[19] H. Rieder, A. Dillhöfer, M. Spies, J. Bamberg, T. Hess, Online monitoring of additive manufacturing processes using ultrasound, in: In 11th European Conference on Non-Destructive Testing (ECNDT), 2014, pp. 6 – 10.

[20] F. Honarvar, A. Varvani-Farahani, A review of ultrasonic testing applications in additive manufacturing: Defect evaluation, material characterization, and process control, Ultrasonics 108 (2020) 106227. doi:https://doi.org/10.1016/j.ultras.2020.106227.

[21] S. Everton, P. Dickens, C. Tuck, B. Dutton, Using laser ultrasound to detect subsurface defects in metal laser powder bed fusion components, Jom 70 (3) (2018) 378–383.

[22] G. Davis, R. Nagarajah, S. Palanisamy, R. A. R. Rashid, P. Rajagopal, K. Balasubramaniam, Laser ultrasonic inspection of additive manufactured components, Int. J. Adv. Manuf. Technol. 102 (5-8) (2019) 2571–2579.

[23] D. Cerniglia, M. Scafidi, A. Pantano, J. Rudlin, Inspection of additive-manufactured layered components, Ultrasonics 62 (2015) 292 – 298. doi:https://doi.org/10.1016/j.ultras.2015.06.001.

[24] M. Roy, K. Walton, J. B. Harley, M. Skliar, Ultrasonic evaluation of segmental variability in additively manufactured metal components, in: 2018 IEEE International Ultrasonics Symposium (IUS), IEEE, 2018, pp. 1–4.

[25] T. Sol, S. Hayun, D. Noiman, E. Tiferet, O. Yeheskel, O. Tevet, Nondestructive ultrasonic evaluation of additively manufactured alsi10mg samples, Addit. Manuf. 22 (2018) 700 – 707. doi:https://doi.org/10.1016/j.addma.2018.06.016.

[26] Y. Jin, E. Walker, H. Heo, A. Krokhin, T.-Y. Choi, A. Neogi, Nondestructive ultrasonic evaluation of fused deposition modeling based additively manufactured 3d-printed structures, Smart Mater. Struct. 29 (4) (2020) 045020. doi:https://doi.org/10.1088/1361-665X/ab74b9.

[27] H. D. I. Abarbanel, R. Brown, J. J. Sidorowich, L. S. Tsimring, The analysis of observed chaotic data in physical systems, Rev. Mod. Phys. 65 (1993) 1331–1392. doi:10.1103/RevModPhys.65.1331.

[28] B. Sherafat, A. Rashidi, Y.-C. Lee, C. R. Ahn, A hybrid kinematic-acoustic system for automated activity detection of construction equipment, Sensors 19 (19) (2019) 4286. doi:10.3390/s19194286.

[29] S. Sandoval, P. L. D. Leon, The instantaneous spectrum: A general framework for time-frequency analysis, IEEE Transactions on Signal Processing 66 (21) (2018) 5679–5693. doi:10.1109/TSP.2018.2869121.

[30] E. Ott, Chaos in Dynamical Systems, 2nd Edition, Cambridge University Press, 2002. doi:10.1017/CBO9780511803260.

[31] H. Kantz, T. Schreiber, Nonlinear Time Series Analysis, 2nd Edition, Cambridge University Press, 2003. doi:10.1017/CBO9780511755798.

[32] S. H. Strogatz, Nonlinear Dynamics and Chaos: With Applications to Physics, Biology, Chemistry, and Engineering, Second Edition, 2nd Edition, CRC Press, 2015.

[33] A. Carrión, V. Genovés, J. Gosálbez, R. Miralles, J. Payá, Ultrasonic signal modality: A novel approach for concrete damage evaluation, Cement and Concrete Research 101 (2017) 25 – 32. doi:10.1016/j.cemconres.2017.08.011.

[34] E. Dehghan-Niri, H. Al-Beer, Phase-space topography characterization of nonlinear ultrasound waveforms, Ultrasonics 84 (2018) 446 – 458. doi:10.1016/j.ultras.2017.12.007.

[35] S. Zamen, E. Dehghan-Niri, Observation and diagnosis of chaos in nonlinear acoustic waves using phase-space domain, Journal of Sound and Vibration 463 (2019) 114959. doi:10.1016/j.jsv.2019.114959.

[36] S. Zamen, E. Dehghan-Niri, Fractal analysis of nonlinear ultrasonic waves in phase-space domain as a quantitative method for damage assessment of concrete structures, NDT & E International 111 (2020) 102235. doi:10.1016/j.ndteint.2020.102235.

[37] S. Zamen, E. D. Niri, Analyzing nonlinear behavior of ultrasound wave in phase-space domain, in: A. L. Gyekenyesi (Ed.), Nondestructive Characterization and Monitoring of Advanced Materials, Aerospace, Civil Infrastructure, and Transportation XIII, Vol. 10971, International Society for Optics and Photonics, SPIE, 2019, pp. 402 – 409. doi:10.1117/12.2514392.

[38] M. T. Rosenstein, J. J. Collins, C. J. De Luca, A practical method for calculating largest lyapunov exponents from small data sets, Physica D: Nonlinear Phenomena 65 (1) (1993) 117 – 134. doi:https://doi.org/10.1016/0167-2789(93)90009-P.

[39] N. H. Packard, J. P. Crutchfield, J. D. Farmer, R. S. Shaw, Geometry from a time series, Phys. Rev. Lett. 45 (1980) 712–716. doi:10.1103/PhysRevLett.45.712.

[40] M. B. Kennel, R. Brown, H. D. I. Abarbanel, Determining embedding dimension for phase-space reconstruction using a geometrical construction, PHYSICAL REVIEW A 45 (1992) 3403–3411. doi:10.1103/PhysRevA.45.3403.

[41] A. M. Fraser, H. L. Swinney, Independent coordinates for strange attractors from mutual information, PHYSICAL REVIEW A 33 (1986) 1134–1140. doi:10.1103/PhysRevA.33.1134.

[42] O. Buck, W. L. Morris, J. M. Richardson, Acoustic harmonic generation at unbonded interfaces and fatigue cracks, Applied Physics Letters 33 (5) (1978) 371–373. doi:10.1063/1.90399.

[43] M. J. Crocker, Handbook of noise and vibration control, John Wiley & Sons, 2007.

[44] T. P. Berndt, R. E. Green, Feasibility Study of a Nonlinear Ultrasonic Technique to Evaluate Adhesive Bonds, Springer US, Boston, MA, 1998.

[45] D. Dutta, H. Sohn, K. A. Harries, P. Rizzo, A nonlinear acoustic technique for crack detection in metallic structures, Structural Health Monitoring 8 (3) (2009) 251–262. doi:10.1177/1475921709102105.

[46] D. Donskoy, A. Sutin, A. Ekimov, Nonlinear acoustic interaction on contact interfaces and its use for nondestructive testing, NDT & E International 34 (4) (2001) 231 – 238. doi:10.1016/S0963-8695(00)00063-3.

[47] L. A. Ostrovsky, Wave processes in media with strong acoustic nonlinearity, The Journal of the Acoustical Society of America 90 (6) (1991) 3332–3337.

[48] T. Chondros, A. Dimarogonas, J. Yao, Longitudinal vibration of a bar with a breathing crack, Engineering Fracture Mechanics 61 (5) (1998) 503 – 518. doi:10.1016/S0013-7944(98)00077-0.

[49] T. Chondros, A. Dimarogonas, J. Yao, Vibration of a beam with a breathing crack, Journal of Sound and Vibration 239 (1) (2001) 57 – 67. doi:10.1006/jsvi.2000.3156.

[50] H. Kantz, A robust method to estimate the maximal lyapunov exponent of a time series, Physics letters A 185 (1) (1994) 77–87. doi:https://doi.org/10.1016/0375-9601(94)90991-1.

[51] R. Sasaki, T. Ogata, Y. Ohara, T. Mihara, K. Yamanaka, Simulation and analysis of subharmonics and tail effect for ultrasonic nondestructive evaluation of closed cracks, Japanese journal of applied physics 44 (6S) (2005) 4389.